Construction and Building Materials 197 (2019) 747–756

Contents lists available at ScienceDirect

Construction and Building Materials

journal homepage: www.elsevier.com/locate/conbuildmat

# Effect of slag, silica fume, and metakaolin on properties and performance of alkali-activated fly ash cured at ambient temperature

Hani Alanazi [a], Jiong Hu [b,*], Yong-Rak Kim [c]

[a] Department of Civil Engineering, University of Nebraska-Lincoln, 362 Whittier Research Center, Lincoln, NE 68583-0856, United States
[b] Department of Civil Engineering, University of Nebraska-Lincoln, 203D Peter Kiewit Institute, Omaha, NE 68182, United States
[c] Department of Civil Engineering, University of Nebraska-Lincoln, 362N Whittier Research Center, Lincoln, NE 68583-0856, United States

## HIGHLIGHTS

- Effect of cementitious additives on alkali-activated fly ash (AAFA) properties was studied.
- Flowability reduced with addition of cementitious additives.
- Only one peak was observed in the heat evolution curve from all AAFA mixtures tested.
- Addition of slag largely changed the porosity and pore size distribution.
- Early strength development improved with addition of metakaolin.

## ARTICLE INFO

*Article history:*
Received 5 April 2018
Received in revised form 14 October 2018
Accepted 22 November 2018

*Keywords:*
Ambient curing
Fly ash
Slag
Silica fume
Metakaolin
Workability
Heat evolution
Mechanical properties
Permeability
Pore structure analysis

## ABSTRACT

Alkali-activated fly ash (AAFA) is usually cured at elevated temperature, which limits its wide field applications. However, several studies have shown that properties of AAFA cured at ambient temperature can be significantly improved by incorporating different cementitious additives. This research investigated the impact of substituting a small portion of fly ash with different potential cementitious additives such as slag, metakaolin, and silica fume on various properties of AAFA mixtures at ambient curing conditions. Toward that end, several experimental observations including workability, geopolymerization heat released, compressive strength, Young's modulus, electrical resistivity, chloride permeability, and pore structure distribution were made. The effects of alkaline solution concentration combined with the different chemical compositions on mechanical properties and permeability characteristics were also investigated. An ordinary Portland cement was also included in the testing program as a comparative reference. Test results showed that the AAFA mixtures exhibited lower heat as compared to ordinary Portland cement mixture, and the results of heat evolution were in line with early-age strength development. The inclusion of metakaolin resulted in a significant improvement in the early strength and stiffness. The inclusion of slag led to the improvement of the mechanical and permeability properties of AAFA cured at ambient temperature, and the effect of sodium silicate (SS) to sodium hydroxide (SH) solution ratio was found to be more profound when the slag was used as an additive. Incorporating silica fume in the AAFA mixtures decreased the mechanical properties and increased the volumetric percentage of large capillary pores.



## 1. Introduction

Concrete is the world's most used construction material, and concrete production is a significant contributor to the global emission of greenhouse gases [1]. The popularity of concrete comes from its cost, mechanical properties, and availability. However, concrete can suffer from premature failure due to physical and chemical attacks. The short- and long-term properties of concrete are mainly controlled by its binder. The most commonly used binder in concrete is ordinary Portland cement (OPC) since its development as a binder over 180 years ago. OPC production consumes a significant quantity of natural resources and releases a large amount of $CO_2$. The production of one ton of OPC emits approximately one ton of $CO_2$ into the atmosphere [2,3]. As a result, OPC production is responsible for 5–7% of the world's $CO_2$ emissions [3,4]. According to United States Environmental

* Corresponding author.
*E-mail addresses:* hani.alanazi@huskers.unl.edu (H. Alanazi), jhu5@unl.edu (J. Hu), yong-rak.kim@unl.edu (Y.-R. Kim).

https://doi.org/10.1016/j.conbuildmat.2018.11.172
0950-0618/

Protection Agency (EPA), $CO_2$ is the primary greenhouse gas, and $CO_2$ contributes to 81% of all United States greenhouse gas emissions in 2014 [5]. The growing awareness on global warming and sustainability issues in the last decades has been increasing and urging the construction industry to explore a green alternative to OPC [6,7]. Another motivation to find alternative to OPC is related to its durability deficiency in certain environments. For instance, OPC concrete largely deteriorates in environmental conditions with high acidity or high sulfate concentrations [8]. For such cases, alternative materials could perform better in aggressive environments and greatly reduce the $CO_2$ emissions in long term.

In recent years, alkali-activated binders have emerged as an environmentally friendly alternative to OPC. Alkali-activated materials (AAM) are generally synthesized by the reaction of aluminosilicate raw materials (e.g., fly ash, slag, and metakaolin) and alkaline solution. The commonly used alkaline solution is a mixture of sodium silicate (SS) and sodium hydroxide (SH) solutions, where the ratio of SS/SH, water to binder ratio (w/b), and concentration of SH are considered as the most critical factors that influence the fresh and hardened properties of AAM [9–11]. Class F fly ash is a suitable aluminosilicate material than the others due to its high content of silica and alumina, low water demand, and worldwide availability [12]. Alkali-activated fly ash (AAFA), one of geopolymers, has several advantages over OPC. For instance, utilizing industrial by-products such as fly ash as aluminosilicate raw materials will have a positive impact on the environment. These impacts include addressing the issues of disposing these industrial by-products in the landfill and reducing the $CO_2$ emissions. $CO_2$ emissions expected from geopolymer are lower by 80% compared to OPC [13], and other researchers reported that geopolymer releases about 26–45% $CO_2$ less than OPC [7,14]. The formation process in AAFA system consists of the dissolution of the aluminosilicate reactants in strong alkali solution, yielding repeated polymeric Si-O-Al-O bonds in amorphous form [15]. The main reaction product in AAFA system is an amorphous aluminosilicate gel known as sodium aluminosilicate hydrate (N-A-S-H) gel, which is clearly different from the main reaction product in OPC known as calcium silicate hydrate (C-S-H) [16].

Previous studies indicated that the chemical reaction, strength development, and permeability of AAFA are largely affected by the solid precursor materials, alkaline solution, and curing process [17,18]. The strength and stiffness development rate of AAFA cured at ambient condition are generally low [1], and an elevated temperature is mostly needed. On the other hand, the permeability of AAFA concrete was found to be higher than the permeability of OPC concrete [19,20]. Many studies have investigated the effect of various parameters on the durability and mechanical properties of AAFA cured at elevated temperature, but there are limited studies on the mechanical properties and permeability of AAFA cured at ambient temperature incorporated with cementitious additives.

AAM made with low calcium fly ash (or class F fly ash) required curing at elevated temperature in order to have acceptable mechanical properties in short- and long-term [21,22]. However, the need for curing at elevated temperature limits its wide construction applications, and addressing this issue is thus crucial for adopting AAM in field applications. The elimination of heat curing process will result in significant cost and energy savings. Being able to circumvent the high permeability and low strength development rate of AAFA cured at ambient temperature will have a significant impact on the adoption of AAFA. In the strive towards improving the AAFA cured at ambient condition, some researchers partially replaced fly ash with other cementitious materials such as slag and OPC in order to accelerate the setting and strength development [23–25]. The addition of calcium source into AAFA system was reported to largely affect the fresh and hardened properties of AAFA due to an additional C-S-H gel formation in the presence of N-A-S-H [26]. Also, increasing the fineness of fly ash was reported to accelerate the geopolymerization process [27], but the approach is neither practical nor cost effective. However, there is limited information in the literature on AAFA incorporated with metakaolin and silica fume [28,29]. Metakaolin and silica fume are different from other pozzolanic materials due to their surface area, fineness, high reactivity, and high-water demand. The inclusion of metakaolin and silica fume in OPC concrete has been proven to improve its permeability.

Incorporating cementitious additives into AAFA is expected to yield various changes in physical and mechanical characteristics due to different chemical reactions among constituents. This study aims to investigate the impact of substituting a small portion of fly ash with different cementitious additives such as slag, metakaolin, and silica fume on workability, geopolymerization heat released, compressive strength, Young's modulus, electrical resistivity, chloride permeability, and pore structure distribution of AAFA mixtures cured at ambient conditions. The effects of binder composition on compressive strength and stiffness development were monitored at different curing ages. The effects of different chemical compositions and concentrations of alkaline solution on the mechanical properties and permeability characteristics of AAFA with different cementitious additives were also investigated.

## 2. Materials and experimental procedures

### 2.1. Materials

The main aluminosilicate source material used in this study to manufacture AAFA mortar is a class F fly ash obtained from Boral, Colorado that complying with ASTM C618 [30]. Commercially available slag, silica fume, and metakaolin complying with ASTM C989, C1240 and C618 [30-32] respectively were used as a partial replacement of fly ash. Slag, silica fume, and metakaolin used in this study were supplied by Skyway Cement Company LLC, GCP Applied Technologies, and Fishstone Studio Inc., respectively. For the purpose of comparison, Type I Portland cement complying to ASTM C150 [33] was also used to prepare the OPC mortar mixture. Type I Portland cement was supplied by Ash Grove Cement Company. The chemical compositions of class F fly ash, slag, silica fume, metakaolin and cement are shown in Table 1. The contents of silica and alumina in metakaolin are approximately 96% of its chemical composition. The silica content in silica fume is approximately 95% of its chemical composition. On the contrary to metakaolin and silica fume, slag contains a high content of calcium oxide. The alkaline solution used in this study was a mixture of SH and SS solutions. SH solution was prepared by dissolving sodium hydroxide pellets with a purity of 98% in distilled water. SH solution of 12 M concentration was kept constant for all mixtures. The chemical compositions of SS solution used in this study are 28% $SiO_2$, 9% $Na_2O$, and 63% water. A locally available fine aggregate that meets ASTM C33 [34] was used to prepare all mortar mixtures.

### 2.2. Mix proportions, mixing, and curing

The mixture proportions of the sixteen AAFA and one OPC mortars are shown in Table 2. The mixture variables include the amount of slag, silica fume, and metakaolin as a replacement of fly ash (by mass), SS/SH ratio, and curing conditions. Mixtures FA1 to FA4 were prepared with only fly ash (as a binding material) to study the effect of SS/SH ratio and curing at elevated and ambient temperature on AAFA system, and these mixtures serve as control mixtures. The AAFA mortar mixtures were designated based on their varying components in the mixture. For instance, FA-2.5SF10 represents a AAFA mixture having the ratio of SS/SH of 2.5 (FA-2.5) and substituting 10% of fly ash by silica fume (SF10). The alkaline solution content in all AAFA mixtures was fixed at 40% of the total binder, and the fine aggregate-to-binder ratio was fixed at 1.0. No extra water or superplasticizer was added to the mixtures. Regarding the parameter (w/b), the mass of water comes from the water contained in the SS solution and SH solution.

The mixing of all mixtures was mechanically performed with an ASTM C305-compliant laboratory mixer [35]. The alkaline solution was prepared 24 h prior to its final use by mixing SS with SH at a designed quantity. To ensure that fly ash is mixed evenly with other additives, the binder and fine aggregates were first dry-mixed for 3 min at a low speed (140 ± 5 rpm). To obtain a uniform and consistent mix, the alkaline solution was then added gradually to the solid ingredients and continued mixing for another 5 min at the same speed of 140 ± 5 rpm. The mixer was stopped in two minutes after adding the alkaline solution, and the mortar was manually mixed with a spatula prior to being placed into molds to ensure the homogeneity of the mixture. The similar procedure was used to mix OPC mortar

**Table 1**
Chemical compositions of class F fly ash, slag, silica fume, metakaolin, and OPC.

| Component% | $SiO_2$ | $Al_2O_3$ | $Fe_2O_3$ | CaO | MgO | $SO_3$ | $Na_2O$ | $K_2O$ | $TiO_2$ | LOI* |
|---|---|---|---|---|---|---|---|---|---|---|
| Fly ash | 56.52 | 22.75 | 4.56 | 8.53 | 2.64 | 0.4 | 0.69 | 1.16 | | 0.35 |
| Slag | 35.9 | 10.08 | 0.51 | 39.8 | 10.75 | 2.601 | 0.335 | 0.369 | 0.499 | |
| Silica fume | 94.49 | 0.07 | 0.1 | 0.5 | 0.62 | 0.11 | 0.09 | 0.54 | | 3.21 |
| Metakaolin | 55.01 | 40.94 | 0.55 | 0.14 | 0.34 | | 0.09 | 0.6 | 0.55 | 1.54 |
| OPC | 21.75 | 5.15 | 3.23 | 63.75 | 1.15 | 1.95 | 0.33 | 0.56 | | 2.08 |

* Loss on ignition.

**Table 2**
Details of mix proportions.

| Mix ID | Specimen designation | Binder proportions (wt%) | | | | | Alkaline solution | Molar ratio | Water to binder | Curing condition |
|---|---|---|---|---|---|---|---|---|---|---|
| | | Fly ash | Slag | Silica fume | Metakaolin | OPC | SS/SH | $Na_2O/SiO_2$ | | |
| FA1 | FA-1 60 °C | 100 | | | | | 1.0 | 0.128 | 0.240 | 60 °C for 24 hrs |
| FA2 | FA-2.5 60 °C | 100 | | | | | 2.5 | 0.099 | 0.231 | 60 °C for 24 hrs |
| FA3 | FA-1 | 100 | | | | | 1.0 | 0.128 | 0.240 | Ambient temperature |
| FA4 | FA-2.5 | 100 | | | | | 2.5 | 0.099 | 0.231 | Ambient temperature |
| FA5 | FA-1S10 | 90 | 10 | | | | 1.0 | 0.132 | 0.240 | Ambient temperature |
| FA6 | FA-2.5S10 | 90 | 10 | | | | 2.5 | 0.102 | 0.231 | Ambient temperature |
| FA7 | FA-1S15 | 85 | 15 | | | | 1.0 | 0.134 | 0.240 | Ambient temperature |
| FA8 | FA-2.5S15 | 85 | 15 | | | | 2.5 | 0.103 | 0.231 | Ambient temperature |
| FA9 | FA-1SF5 | 95 | | 5 | | | 1.0 | 0.124 | 0.240 | Ambient temperature |
| FA10 | FA-2.5SF5 | 95 | | 5 | | | 2.5 | 0.096 | 0.231 | Ambient temperature |
| FA11 | FA-1SF10 | 90 | | 10 | | | 1.0 | 0.120 | 0.240 | Ambient temperature |
| FA12 | FA-2.5SF10 | 90 | | 10 | | | 2.5 | 0.093 | 0.231 | Ambient temperature |
| FA13 | FA-1MK5 | 95 | | | 5 | | 1.0 | 0.128 | 0.240 | Ambient temperature |
| FA14 | FA-2.5MK5 | 95 | | | 5 | | 2.5 | 0.099 | 0.231 | Ambient temperature |
| FA15 | FA-1MK10 | 90 | | | 10 | | 1.0 | 0.127 | 0.240 | Ambient temperature |
| FA16 | FA-2.5MK10 | 90 | | | 10 | | 2.5 | 0.098 | 0.231 | Ambient temperature |
| OPC | OPC | | | | | 100 | | | 0.400 | Moisture |

with water-to-cement ratio (w/c) of 0.40. A w/c of 0.40 was chosen for this study to ensure a workable mixture with moderate strength. The OPC mortar mixture had the same amount of aggregate and binder as AAFA mixture had.

Fresh AAFA and OPC mortars were cast in 50 mm cubic molds and in cylindrical molds of 100 mm in diameter and 200 mm in height. FA1 and FA2 specimens were sealed in zipper plastic bags and cured at 60 °C for 24 h in a laboratory oven, and then demolded and stored in a controlled environment with temperature of 23 ± 2 °C and relative humidity of 60% until the day of testing. Mixtures FA3 to FA16 were cured at ambient temperature (23 ± 2 °C) for 24 h, then demolded and sealed in plastic bags until the testing date. OPC specimens had different curing regime where specimens after casting were stored at room temperature (23 ± 2 °C) and sealed by plastic sheets to prevent excessive moisture loss. After 24 h, OPC mortar specimens were demolded and placed in limewater until testing.

### 2.3. Test methods

Concrete requires an appropriate flowability for adequate consolidation, as well as cohesion to ensure concrete to be transported without any segregation issue. The effect of different variables on the workability of fresh AAFA mixtures was measured in terms of flow percentage in accordance with ASTM C1437 [36]. The flow test was performed immediately after mixing. Each flow percentage value was the average of two mixes.

The heat evolution of AAFA and OPC mixtures was measured by an isothermal calorimeter at a constant temperature of 23 °C. The isothermal calorimetry tests were conducted to study the effect of different additives on early-age geopolymerization. The samples were immediately placed into the calorimeter after mixing, then the readings were taken every one minute for 72 h.

To measure the compressive strength of each mortar mixture, 50 mm cubic specimens were used following the ASTM C109/109 M [37]. Compressive strength tests were conducted at 1, 3, 7, and 28 days in order to monitor the strength growth. The dynamic modulus of elasticity was determined by the impact resonance frequency method with the longitudinal mode in accordance with the ASTM C215 [38] using a E-modumeter system. This test was used to observe the stiffness development at different curing times (i.e., 1, 3, 7, and 28 days) from the same specimens since the test is nondestructive. The results from the resonance method are considered more reproducible than the destructive tests since the tests can be performed on the same specimens. The compressive strength and dynamic modulus tests were performed on three specimens for each mix at different curing times (i.e., 1, 3, 7, and 28 days) and the average values were reported.

Permeability tests were conducted on the specimens (100x200 mm cylinders) after 28 days of curing. The surface resistivity tests were performed on fully saturated specimens according to the AASHTO TP 95-11 [39]. The 4-pin Wenner probe array was used to measure the electrical resistivity using a Resipod model 38 mm device from Proceq. The test involves applying an alternative current potential at the outer pins. A current is generated to flow through the specimen, then the drop in resultant potential is measured by the inner pins and used to calculate the resistivity. This test can be related to the pore microstructure and the specimen permeability. Another test to evaluate permeability of concrete or mortar is the rapid chloride permeability test (RCPT), ASTM C1202 [40]. The cylinder specimens used in this test were cut from the middle of 100 × 200 mm cylinders with a diamond saw into discs with 100 mm in diameter and 50 mm thick. The specimens were coated on the sides with an epoxy resin. After coating, the specimens were vacuum saturated and then placed between two testing cells. One cell was filled with 0.3 M NaOH and the other cell was filled with 3% NaCl solution. A 60 V DC was applied between the two cut faces, then the current passing through the specimens was measured every minute, and the total charge (in Coulombs) passing through the specimen after 6 h of testing was obtained.

Since the RCPT and surface resistivity tests used to study the permeability of AAFA are somewhat controversial due to the existence of metallic ions in the pore solution [20,41], which may mislead the realistic phenomenon, another testing method was included to characterize the effects of cementitious additives on the pore structure and porosity of AAFA. The porosity and pore size distribution of AAFA pastes were measured by Mercury Intrusion Porosimetry (MIP) using a Quantachrome PoreMaster 60 with a maximum intruding pressure of 420 MPa corresponding to a minimum pore size of 3 nm. Specimens with a size of approximately 1.0 $cm^3$ were cut from the middle of 100x200 mm cylinders using a diamond saw. After cutting, the specimens were immersed in ethanol for 24 h to cease any further chemical reaction, then the specimens were dried in an oven at 70 °C for 4 h prior to MIP testing.

## 3. Results and discussion

### 3.1. Flow characteristics

The effect of cementitious additives and SS/SH ratios on the flowability of AAFA mixtures is shown in Fig. 1. The results were compared with the OPC mortar and control AAFA mortars (FA-1

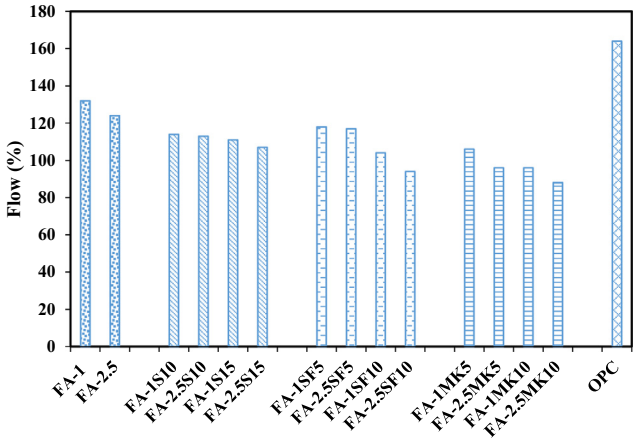


**Fig. 1.** Flow characteristics of AAFA and OPC mortars.

and FA-2.5) made with only fly ash as the binder. The results indicated that the flow behavior of AAFA mortars was influenced by the inclusions of slag, silica fume, and metakaolin in the binder and the ratio of SS/SH. FA-1 and FA-2.5 designed with fly ash alone showed the highest flow values compared to other AAFA mortars, which seems due to the spherical shape and slow chemical reaction of fly ash particles [1]. The flow values of all AAFA mortars decreased with the increase of slag, silica fume, and metakaolin content in the binder. The decrease in the flow of AAFA mixtures containing silica fume or metakaolin might be attributed to the high surface areas and smaller particle sizes, while the reduction in flow of AAFA mixtures containing slag might be related to the rougher surface texture and rapid reaction due to the high calcium content, which agrees with other relevant studies [42,43]. FA-2.5MK10 mixture, where fly ash was replaced with 10% of metakaolin and activated with SS/SH ratio of 2.5, showed the lowest flowability. No segregation or bleeding was observed during mixing or testing.

The flow behavior of AAFA was reported to be influenced by the SH concentration and the ratio of SS/SH [10]. The alkaline solution used in this study was a mixture of SS and SH, and the ratio of SS/SH was varied between 1.0 and 2.5. AAFA mixtures were found to be more cohesive and sticky than OPC mixture since the alkaline solutions are more viscous than water. It can be seen in Fig. 1 that the flow values of all AAFA mixtures decreased with an increase of SS/SH ratio from 1.0 to 2.5 due to the increased sodium content in the alkaline solution.

### 3.2. Heat evolution

The influence of cementitious additives on the heat evolution of AAFA mixtures is shown in Fig. 2. Also, the heat evolution curve for OPC with w/c of 0.40 is illustrated in Fig. 2(a) as a comparison. The geopolymerization process is a complex process that consists of three steps: dissolution, precipitation, and polycondensation, and the three steps occur almost simultaneously [44]. The geopolymerization is an exothermic process which is greatly influenced by the chemical compositions of the binders and alkaline solution. As shown in Fig. 2, the heat evolution curves of all AAFA mixtures displayed generally a similar behavior, i.e., only one peak was observed. The peak within the first three hours upon the completion of mixing corresponds to the dissolution and precipitation of particles as shown in Fig. 3. The first heat release peak of OPC mix was much higher than that of AAFA mixes. After a few hours upon the completion of all AAFA mixing, the process went into a thermally steady state. The smallest peak was observed from FA-1 that contains fly ash alone as its binder, which was reported to be related to the low glass content and calcium ions of fly ash [45]. Fig. 2(d) shows the peaks resulting from AAFA mixtures with

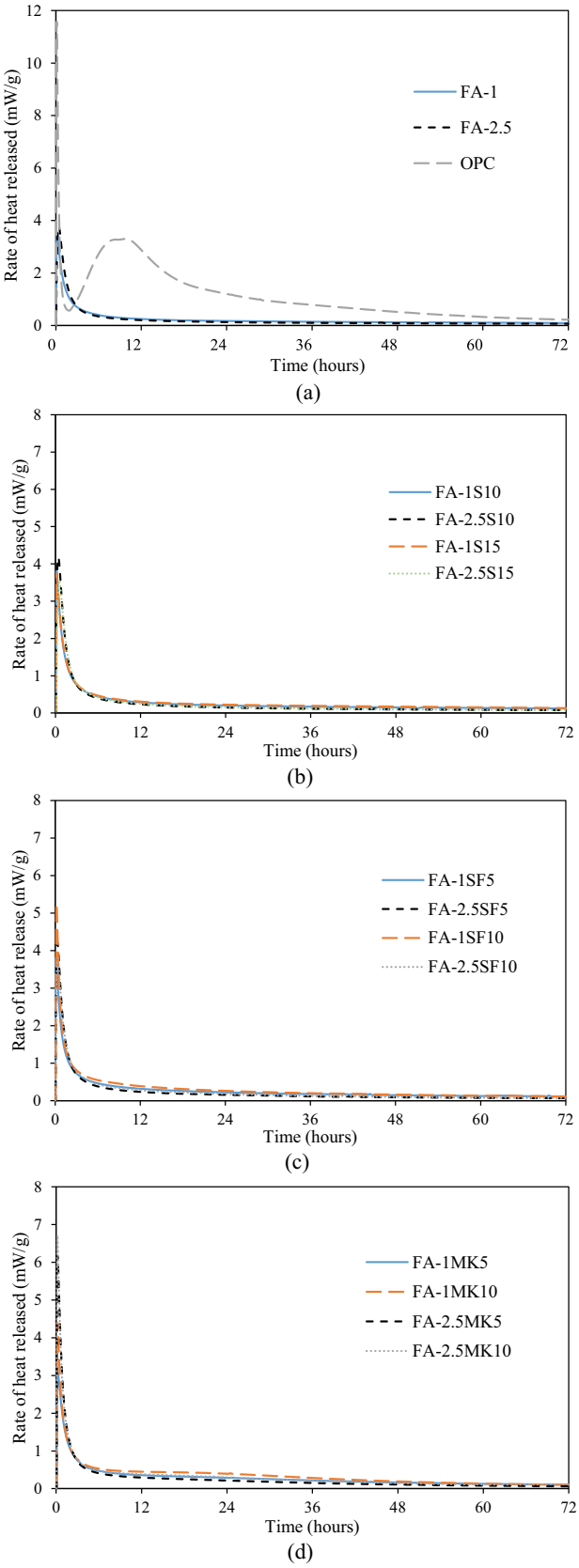


**Fig. 2.** Heat evolution comparison. (a) Reference mixes, (b) Effect of slag and SS/SH, (c) Effect of silica fume and SS/SH, and (d) Effect of metakaolin and SS/SH.

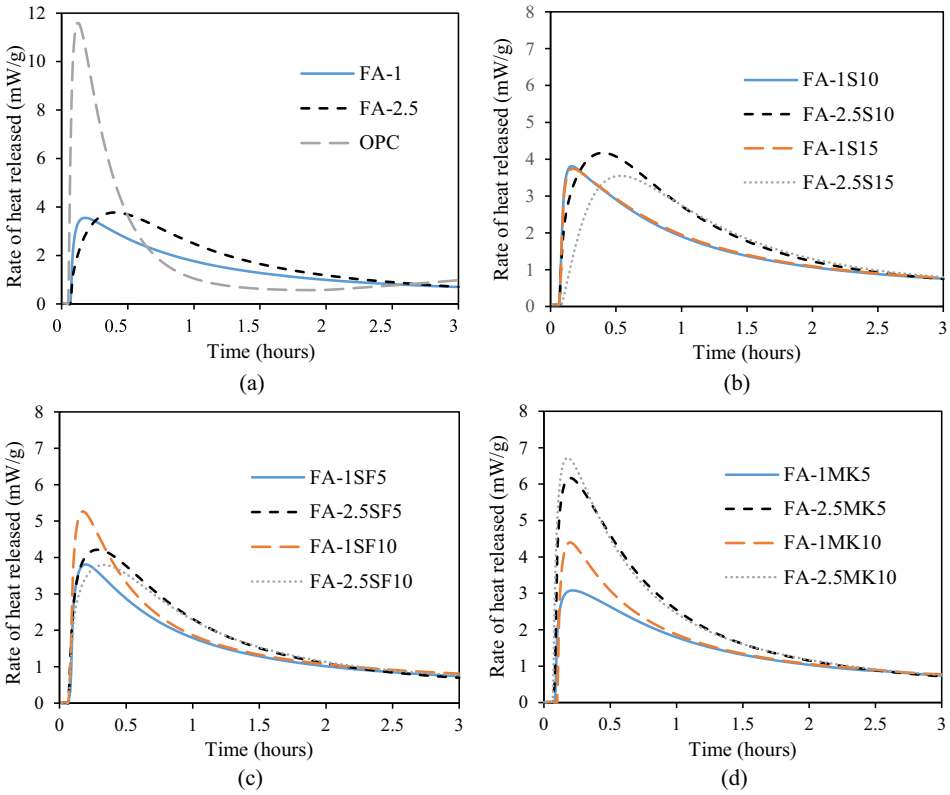


**Fig. 3.** Heat evolution comparison during the first three hours. (a) Reference mixes, (b) Effect of slag and SS/SH, (c) Effect of silica fume and SS/SH, and (d) Effect of metakaolin and SS/SH.

metakaolin. They were the highest among others, and the highest peaks are attributed to high reactivity of metakaolin with alkaline solution. Metakaolin was reported to be more reactive than fly ash during the geopolymerization process [46,47]. When SS/SH ratio varied between 1.0 and 2.5, the behavior of heat release and sharpness were slightly different, as shown in Fig. 3.

### 3.3. Compressive strength and dynamic modulus of elasticity

The influence of curing conditions and SS/SH ratio on the time-dependent compressive strength of AAFA mixtures are shown in Fig. 4(a). Also, the compressive strength of OPC specimen over time was presented for a comparison purpose. The strength development rate of AAFA greatly depends on the geopolymerization degree, which relies on the extent of dissolved elements from the source materials. As can be seen, the AAFA specimens cured at ambient temperature gained a very low strength after one day of curing, and their 3-day strengths were between 10 MPa and 14 MPa. However, the AAFA specimens cured at 60 °C for 24 h displayed a much higher early strength at approximately 40 MPa after only one day of curing due to the increase in the degree of geopolymerization, i.e., more formation of reaction products. The AAFA specimens cured at elevated temperature gained around 90% of its 28-day strength after only one day. The 28-day compressive strength of the AAFA specimens cured at an elevated temperature was comparable to the compressive strength of OPC specimen.

Since the different AAFA mixes were blended with a similar alkaline solution, any change in the strength development rate would be related to changes in the amount of silicate, alumina, and calcium elements in the source materials. The results of compressive strength of AAFA mortar, where its fly ash was partially replaced with 10% and 15% of slag, are illustrated in Fig. 4(b). As the amount of slag which contains a high portion of CaO increased, the compressive strength increased in both SS/SH ratios (i.e., 1.0 and 2.5). The specimens with 10% and 15% slag replacement exhibited higher compressive strength than those specimens with the fly ash alone. This indicates that the presence of slag in the mixture would modify the microstructure by forming another reaction products such as C-S-H gel along with N-A-S-H gel [45], which would consequently improve the mechanical properties of AAFA mixture. This result agrees with a previous study that investigated microstructural changes from incorporation of slag in AAFA [48]. Among the four cases with slag replacement, FA-1S15 specimen cured at ambient temperature achieved the highest compressive strength (i.e., 47.1 MPa) at 28 days. The effect of SS/SH ratios on the compressive strength was also obvious. It was observed that mixtures with SS/SH ratio of 1.0 generally exhibited higher compressive strength than those with SS/SH ratio of 2.5, and this trend was more evident with an increased curing time.

Fig. 4(c) presents the effect of silica fume inclusions on the compressive strength development of the AAFA mortars at 1, 3, 7, and 28 days. As the silica fume content increased from 5% to 10%, the compressive strength decreased. One plausible reason is likely due to the very low $Al_2O_3$ and CaO content, as presented in Table 1. The addition of silica fume leads to the reduction in the solution alkalinity which in turn lower the dissolution of fly ash particles. The 28-day compressive strength of the AAFA specimens containing silica fume was lower compared to the AAFA specimens with fly ash alone. However, the effect of silica fume associated with alkali-activated precursor could be dependent on curing condition, as other researchers observed an increase in the compressive strength when AAFA containing silica fume cured at elevated temperatures [49,50], which was not evaluated in this study.

The development of compressive strength of AAFA specimens with metakaolin and different chemical compositions of the alkaline solutions is shown in Fig. 4(d). In general, the AAFA mixtures

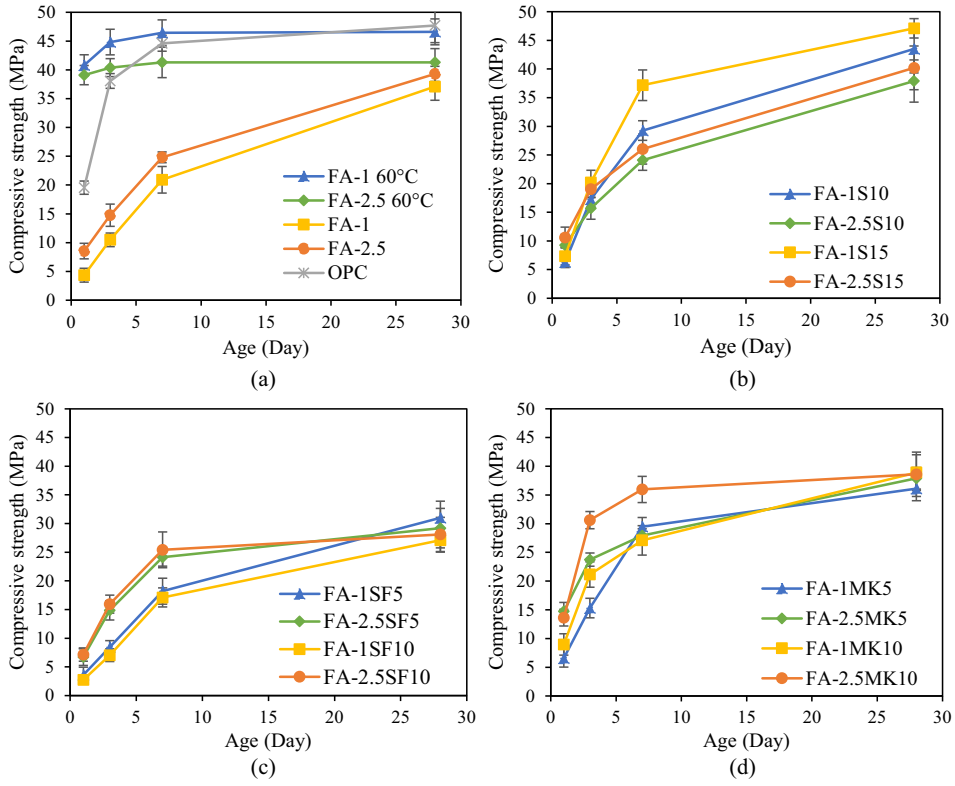


**Fig. 4.** Compressive strength development. (a) OPC and effect of curing conditions and SS/SH, (b) Effect of slag and SS/SH, (c) Effect of silica fume and SS/SH, and (d) Effect of metakaolin and SS/SH.

with metakaolin gained higher early strength than other AAFA mixtures with/without slag or silica fume. This could be attributed to the fact that the aluminum content of metakaolin, as presented in Table 1, was higher than fly ash. Higher alumina content results in a lower ratio of silica to alumina (Si/Al), which would enhance the geopolymerization process and subsequently contribute to high early compressive strength. When 10% of fly ash was replaced with metakaolin with SS/SH ratio of 2.5, the compressive strength significantly increased from 14.76 MPa to 30.62 MPa at 3-day curing. Also, as the replacement ratio of the metakaolin increased from 5% to 10% with the SS/SH ratios of 1.0 and 2.5, the 3-day compressive strength increased from 15.31 MPa to 21.15 MPa and 23.75 MPa to 30.62 MPa, respectively. However, the 28-day compressive strength of AAFA with metakaolin or silica fume did not vary significantly.

Fig. 5 shows the relation between compressive strength and cumulative heat release at 24 h and 72 h. The mixes made with SS/SH ratio of 1.0 displayed higher cumulative heat release than those made with SS/SH ratio of 2.5 regardless of the binder. This could be attributed to the increase in $Na_2O$ content, which lead to a higher heat release [51]. As can be seen in Fig. 5a and b, there is no strong relation between strength development and cumulative heat for AAFA. AAFA mixes containing metakaolin presented higher cumulative heat and strength at 24 h and 72 h comparing to other AAFA mixes.

Dynamic modulus of elasticity is a parameter used to monitor the stiffness development over time. The moduli of elasticity of all AAFA specimens are shown in Fig. 6. The measured dynamic moduli of AAFA mixtures ranged between 14 GPa and 22 GPa, whereas OPC specimen had a dynamic modulus of 32.3 GPa. The low modulus of AAFA mixtures is related to the lower modulus of its paste as compared to the OPC paste since both AAFA and OPC mixtures have similar amount and type of aggregate. These

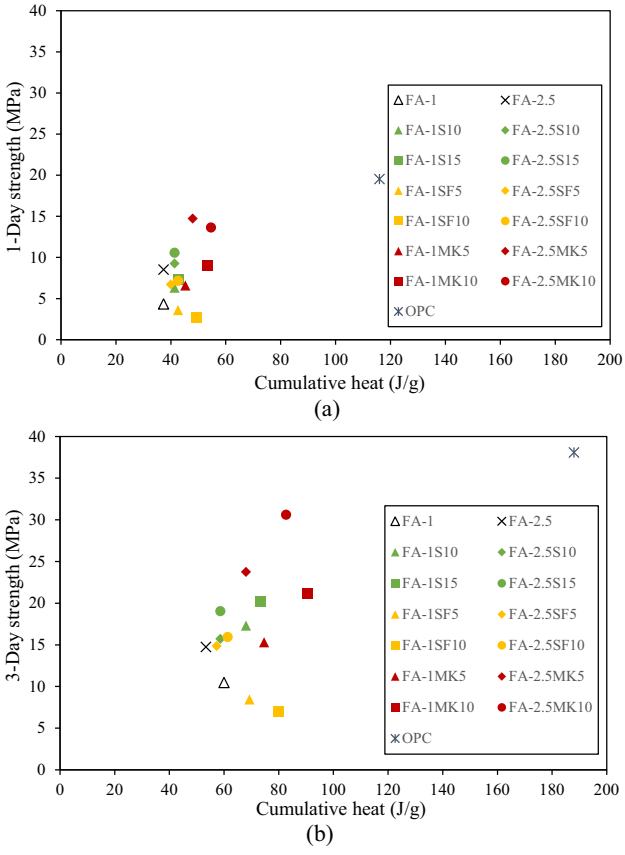


**Fig. 5.** Relations between compressive strength and cumulative heat. (a) 1-Day strength vs. cumulative heat and (b) 3-Day strength vs. cumulative heat.

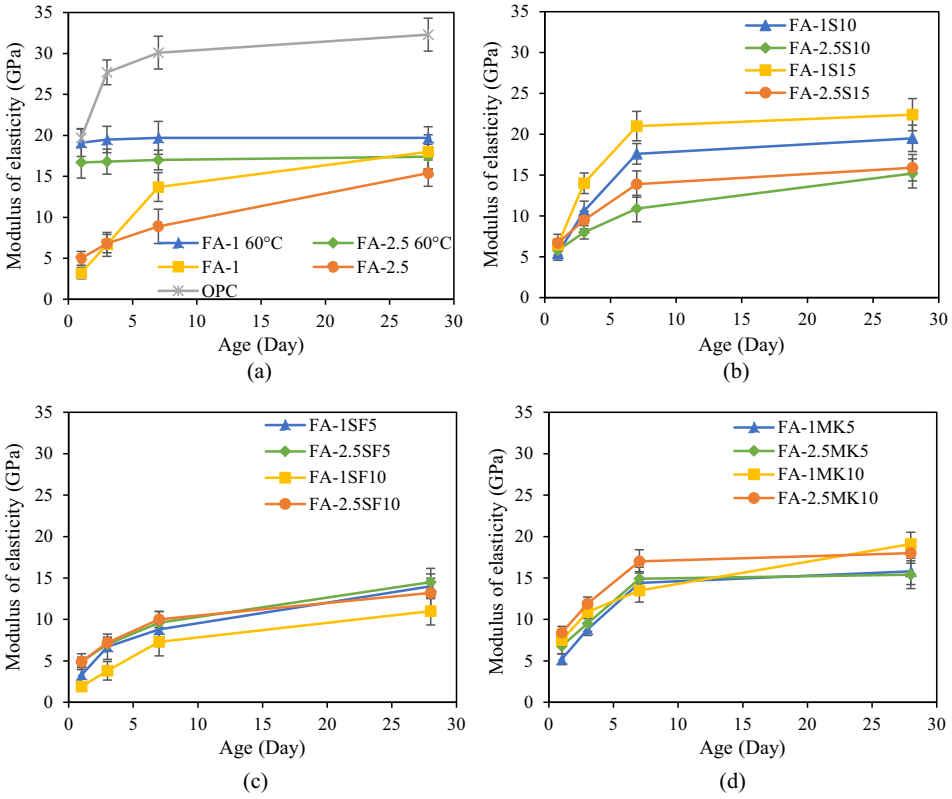


**Fig. 6.** Dynamic modulus of elasticity development. (a) OPC and effect of curing conditions and SS/SH, (b) Effect of slag and SS/SH, (c) Effect of silica fume and SS/SH, and (d) Effect of metakaolin and SS/SH.

results are consistent with the findings in previous studies [2,52]. At a similar strength level, the modulus of elasticity of OPC concrete is approximately 50% higher than that of AAFA concrete [2]. Similar to compressive strength, the effect of cementitious additives on stiffness exhibited the same trend. The addition of silica fume showed a drop in the modulus, and the inclusion of metakaolin slightly improved the stiffness and increased the modulus development rate. The inclusion of slag showed the largest effect on the stiffness. Varying the ratio of SS/SH, while keeping other variables constant, showed a great impact on the modulus of elasticity of the AAFA specimens with slag, while mixtures with silica fume or metakaolin did not show significant changes.

### 3.4. Surface resistivity and RCPT

Surface resistivity tests were performed on saturated AAFA and OPC mortars after 28-day curing and the results are shown in Fig. 7. Each surface resistivity value was the average of three specimens. Surface resistivity depends on the volume, size, and connectivity of pores [53], and a higher amount of metallic ions in the pore solution would reduce the surface resistivity. As can be seen, varying the SS/SH from 2.5 to 1.0 for specimens cured at an elevated temperature led to a significant increase in the surface resistivity which is consistent with results from the compressive strength test. The slag substitution rate with SS/SH ratio of 1.0 made a spectacular contribution to the surface resistivity values of AAFA mortars compared to OPC mix and AAFA mixes cured at an ambient temperature with/without silica fume or metakaolin. The highest surface resistivity recorded was 5.75 kΩ-cm, which is an indication of dense microstructure due to the formation of additional C-S-H and more refined pore networks. Fly ash partially replaced with metakaolin resulted in a drop in the electrical resistivity, and one possible explanation of this is the high conductivity of aluminum ions in the pore solution. Metakaolin has a higher aluminum content comparing to slag and silica fume, which could lead to the decrease in the surface resistivity. However, further study is needed to evaluate the effect of metakaolin on the permeability of AAFA. AAFA specimens incorporated with silica fume exhibited an increase in the surface resistivity compared to the AAFA containing only fly ash and cured at the ambient condition, and this is related to the reduction in the permeability of the paste. The increase in the surface resistivity for specimens containing silica fume may be related to the decrease of free metallic ions (i.e., $Na^+$) in the pore solution due to the high content of $SiO_2$ in silica fume. The reaction between $SiO_2$ and $Na_2O$ in the alkaline solution

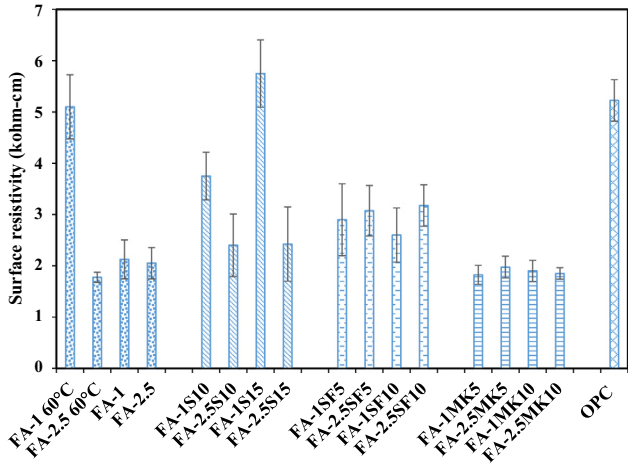


**Fig. 7.** Surface resistivity results of AAFA and OPC mortars.

could lead to the decrease of conductivity and increase of surface resistivity [41]. However, no significant variation in the electrical resistivity yielded due to the variation in SS/SH ratios for AAFA specimens with silica fume or metakaolin.

The RCPT tests, which is considered one of the most commonly used test to study the durability of mortar and concrete [54], were conducted on vacuum saturated specimens at the age of 28 days according to ASTM C1202 and AASHTO T259. Only two mixes were successfully tested (FA-1 60 °C and OPC) because other AAFA mixes drew excessive current (heat) due to the porosity of the microstructure of the paste and the chemical composition of pore solution. The charge passed in the FA-1 60 °C and OPC mortars were 3304 and 5225 Coulombs, respectively. The RCPT results revealed the large influence of curing condition and SS/SH ratio on the permeability of AAFA. The initial current of AAFA containing 15% slag with SS/SH ratio of 1.0 was 205 mA which was slightly lower than OPC initial current, but the current kept increasing until it stopped after 62 min as the current exceeded the safe limit (500 mA). Similar results were also observed from other studies [20,41] where RCPT was conducted to assess the permeability of AAFA materials.

### 3.5. Porosity and pore structure analysis

The influence of SS/SH ratios and cementitious additives on microstructure of AAFA were studied by measuring the distribution of pore size and porosity using MIP. Moreover, OPC was examined to study the difference of the pore size distribution and porosity between AAFA and OPC. Fig. 8 shows the curves of cumulative intrusion volume and pore diameters of FA-1 60 °C, FA-2.5 60 °C, FA-1S15, FA-2.5SF5, FA-2.5MK10, and OPC. The AAFA mixtures designed with fly ash alone at the two different SS/SH ratios showed similar behavior with higher volume of mercury intrusion compared to other AAFA mixtures. In Fig. 8, it is clear that the mercury intrusion into AAFA mixes with slag, silica fume, and metakaolin is very different, and this different behavior would be related to the change in the chemical components of the initial source material. The cumulative mercury volume intruded in the AAFA mixture with slag significantly decreased, while the addition of silica fume and metakaolin slightly lowered the cumulative pore volumes. The more evident change found from the mixture with slag is likely due to the refinement of the pore structure, which is to be discussed later.

The total porosity of the six mixtures was calculated from the cumulative intruded mercury volume at the maximum pressure, and the results are illustrated in Fig. 9. Unlike in OPC, the effect of particle size of different supplemental cementitious materials

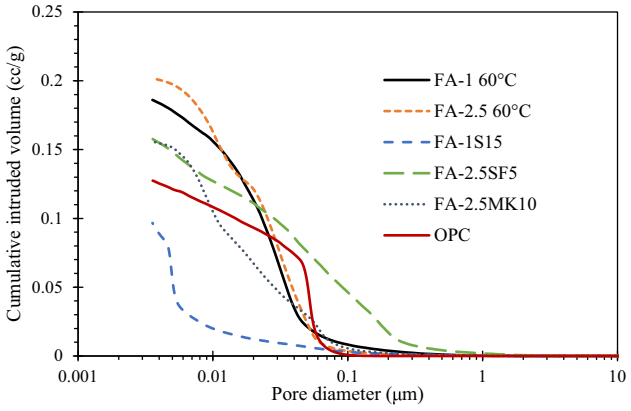


**Fig. 8.** Pore size distribution cumulative curves.

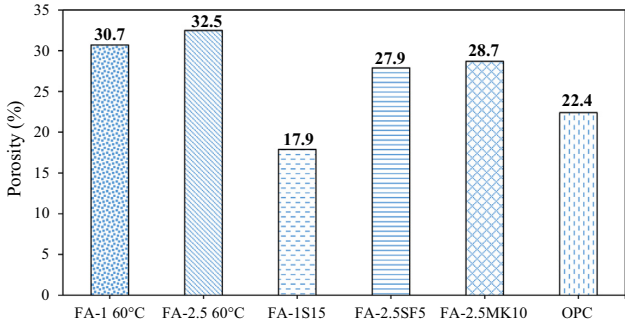


**Fig. 9.** Porosity of AAFA and OPC pastes.

on pore size distribution was not clearly observed in geopolymer mixes, which is likely due to the different reaction kinetics in geopolymer comparing to OPC. The change of element content with the incorporation of other cementitious additives could have a dramatic impact on the reaction in geopolymer and the resulting pore structure. As shown, adding slag led to the reduction of porosity from 30.7% to 17.9%. The significant reduction in the porosity of AAFA with slag, although further study and examination is necessary, might be related to the additional formation of C-S-H gel through activation of slag, which could result in refining of pore structure. In an attempt to further analyze the effects of additives and SS/SH ratios on pore structure, the pore volume distribution of the five mixtures was quantified and its results are shown in Fig. 10. As shown, the measured pores were classified into five groups [55]: pore size over 5 μm as macro pores, pore size from 100 nm to 5 μm as large capillary pores, pore size from 50 to 100 nm as middle capillary pores, pore size from 10 nm to 50 nm as meso-pores, and pore size smaller than 10 nm as gel micropores. The volumetric percentages of pores did not change significantly by varying the ratio of SS/SH. As shown in Fig. 10, the volumetric percentages of pores ranging between 10 and 50 nm were 72% and 69% for FA-1 60 °C and FA-2.5 60 °C, respectively. It was found that 79% of pores in AAFA with slag is in a range of 10 nm and smaller, whereas only 16% of measured pores is in this range for the mixture with fly ash alone at the same SS/SH ratio. This comparative result implies that the formation of C-S-H through activation of slag in AAFA filled most of the capillary pores. The observation is consistent with previous studies [26,45] where slag, which is rich in calcium comparing to fly ash, leads to the formation of C-S-H gel in geopolymer. According to Table 1, CaO accounted for 39.8% and 8.53% of the slag and fly ash respectively used in this study, which apparently leads to a different reaction kinetics. The volumetric percentages of pores in the AAFA with metakaolin were 33% gel micro-pores, 48% meso-pores, 15% middle capillary pores, 4% large capillary pores, and less than 0.1% of

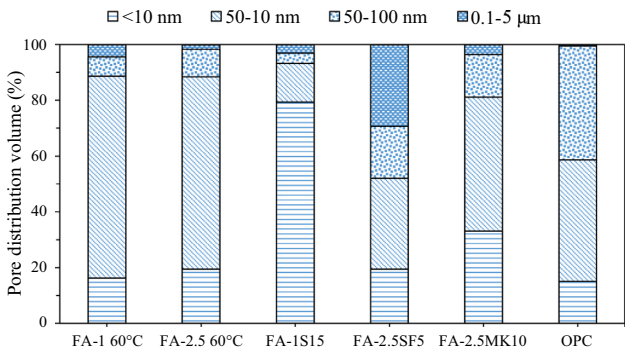


**Fig. 10.** Pore volume distribution.

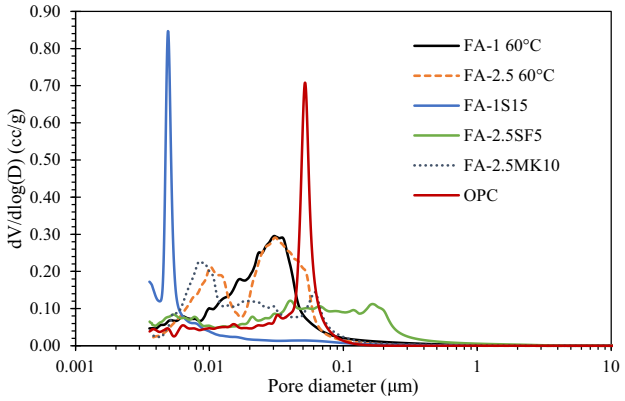


**Fig. 11.** Pore size distribution differential curves.

macro pores, respectively. The inclusion of silica fume in AAFA increased the large capillary pores and decreased the mesopores. This could be attributed to the increase of Si/Al because of a high percentage of $SiO_2$ content in silica fume. The decreased Al content resulting from the substitution of silica fume for fly ash is insufficient for the formation of aluminosilicate gel, which in turn increases the capillary pores. Similar finding was also reported by Lee et al. [56]. The volumetric percentages of pores in the OPC were 15% gel micro-pores, 43.5% meso-pores, 40% middle capillary pores, 0.5% large capillary pores, and less than 0.1% of macro pores, respectively.

Fig. 11 shows the differential pore distribution curves from the six mixtures. The highest peak in the differential curves are known as the critical pore diameter which has been reported to largely influence the permeability and diffusion characteristics of traditional cement materials [57,58]. From the analysis result, the critical pore diameters were 30 nm, 31 nm, 5 nm, 40 nm, 8.5 nm, and 51.9 nm for FA-1 60 °C, FA-2.5 60 °C, FA-1S15, FA-2.5SF5, FA-2.5MK10, and OPC, respectively. The addition of slag and metakaolin into AAFA mixes strongly led to a reduction in the critical pore size, while the addition of silica fume had a negative influence on the critical pore diameter, which is consistent with the results from mechanical properties. Varying the ratio of SS/SH in the mixes containing only fly ash did not significantly change the critical pore size.

## 4. Conclusions

This study experimentally investigated the feasibility of improving early-age properties and strength development of AAFA cured at ambient condition by partially replacing fly ash with different cementitious additives such as slag, silica fume, and metakaolin at varying alkaline solution concentrations. The following conclusions can be drawn from test results and analyses:

- As the additive replacement rate increased, the flowability of all AAFA mixtures reduced. The flowability of AAFA mortars decreased with the increased SS/SH ratio from 1.0 to 2.5.
- Calorimetry test results showed only one peak in the heat evolution curve of AAFA mixtures with additives compared to OPC which presented multiple peaks. The results of heat evolution were in line with early-age strength.
- The addition of slag led to the improvement of the mechanical and permeability properties of AAFA cured at ambient temperature, and the effect of SS/SH ratio was found to be more noticeable when the slag was used as an additive.
- The partial replacement of fly ash with slag dramatically influenced the porosity and pore volume distribution. The porosity and critical pore diameters significantly decreased by the inclusion of slag, which could be attributed to denser microstructure achieved from the formation of additional C-S-H through activation of slag.
- Incorporating silica fume in the AAFA mixtures decreased the mechanical properties and increased the volumetric percentage of large capillary pores.
- Increasing the aluminum content in the binder composition by partially substituting fly ash with metakaolin significantly enhanced the strength development rate (i.e., the 3-day strength increased from 14 MPa to 30 MPa).
- The two different SS/SH ratios used in the study did not present any noticeable effect on the 28-day compressive strength and stiffness of AAFA mixtures with silica fume or metakaolin.

## Conflict of interest

None declared.

## Acknowledgements

The authors are grateful for the financial support received from the National Science Foundation (Grant No. CMMI-1635055). Hani Alanazi would like to acknowledge the financial support from Majmaah University, Saudi Arabia.

## References

[1] P. Nath, P.K. Sarker, Effect of GGBFS on setting, workability and early strength properties of fly ash geopolymer concrete cured in ambient condition, Constr. Build. Mater. 66 (2014) 163–171.
[2] A.M. Fernandez-Jimenez, A. Palomo, C. Lopez-Hombrados, Engineering properties of alkali-activated fly ash concrete, ACI Mater. J. 103 (2) (2006) 106.
[3] C. Meyer, The greening of the concrete industry, Cem. Concr. Compos. 31 (8) (2009) 601–605.
[4] M.B. Ali, R. Saidur, M.S. Hossain, A review on emission analysis in cement industries, Renew. Sustain. Energy Rev. 15 (5) (2011) 2252–2261.
[5] U.S. EPA. Inventory of U.S. greenhouse gas emissions and sinks: 1990–2014. EPA 430-R-16-002. U.S. Environmental Protection Agency, 2016. [Online]. Available: www.epa.gov/climatechange/ghgemissions/usinventoryreport.html.
[6] M. Schneider, M. Romer, M. Tschudin, H. Bolio, Sustainable cement production—present and future, Cem. Concr. Res. 41 (7) (2011) 642–650.
[7] G. Habert, J.D. De Lacaillerie, N. Roussel, An environmental evaluation of geopolymer based concrete production: reviewing current research trends, J. Cleaner Prod. 19 (11) (2011) 1229–1238.
[8] M.C. Juenger, F. Winnefeld, J.L. Provis, J.H. Ideker, Advances in alternative cementitious binders, Cem. Concr. Res. 41 (12) (2011) 1232–1243.
[9] A.M. Mustafa Al Bakri, H. Kamarudin, M. Bnhussain, A.R. Rafiza, Y. Zarina, Effect of $Na_2SiO_3$/NaOH ratios and NaOH molarities on compressive strength of fly-ash-based geopolymer, ACI Mater. J. (2012) 109(5).
[10] A.I. Laskar, R. Bhattacharjee, Rheology of fly-ash-based geopolymer concrete, ACI Mater. J. 108 (5) (2011).
[11] V.F. Barbosa, K.J. MacKenzie, C. Thaumaturgo, Synthesis and characterization of materials based on inorganic polymers of alumina and silica: sodium polysialate polymers, Int. J. Inorg. Mater. 2 (4) (2000) 309–317.
[12] P. Nath, P.K. Sarker, Use of OPC to improve setting and early strength properties of low calcium fly ash geopolymer concrete cured at room temperature, Cem. Concr. Compos. 55 (2015) 205–214.
[13] P. Duxson, J.L. Provis, G.C. Lukey, J.S. Van Deventer, The role of inorganic polymer technology in the development of 'green concrete', Cem. Concr. Res. 37 (12) (2007) 1590–1597.
[14] Witherspoon R, Wang H, Aravinthan T, Omar T. Energy and emissions analysis of fly ash based geopolymers. SSEE 2009: Solutions for a Sustainable Planet. 2009:311.
[15] J. Davidovits, Geopolymer, Green Chemistry and Sustainable Development Solutions: Proceedings of the World Congress Geopolymer 2005, Geopolymer Institute, 2005.
[16] J.L. Provis, J.S. Van Deventer (Eds.), Geopolymers: Structures, Processing, Properties and Industrial Applications, Elsevier, 2009.
[17] E.I. Diaz, E.N. Allouche, S. Eklund, Factors affecting the suitability of fly ash as source material for geopolymers, Fuel 89 (5) (2010) 992–996.
[18] K. Wang, S.P. Shah, A. Mishulovich, Effects of curing temperature and NaOH addition on hydration and strength development of clinker-free CKD-fly ash binders, Cem. Concr. Res. 34 (2) (2004) 299–309.
[19] J. Wongpa, K. Kiattikomol, C. Jaturapitakkul, P. Chindaprasirt, Compressive strength, modulus of elasticity, and water permeability of inorganic polymer concrete, Mater. Des. 31 (10) (2010) 4748–4754.

[20] D.W. Law, A.A. Adam, T.K. Molyneaux, I. Patnaikuni, A. Wardhono, Long term durability properties of class F fly ash geopolymer concrete, Mater. Struct. 48 (3) (2015) 721–731.
[21] B.V. Rangan, Low-calcium fly ash-based geopolymer concrete, Research report GC4, Faculty of Engineering, Curtin University of Technology, 2008.
[22] A. Fernández-Jiménez, I. Garcia-Lodeiro, A. Palomo, Durability of alkali-activated fly ash cementitious materials, J. Mater. Sci. 42 (9) (2007) 3055–3065.
[23] L. Assi, S. Ghahari, E.E. Deaver, D. Leaphart, P. Ziehl, Improvement of the early and final compressive strength of fly ash-based geopolymer concrete at ambient conditions, Constr. Build. Mater. 123 (2016) 806–813.
[24] P. Nath, P.K. Sarker, V.B. Rangan, Early age properties of low-calcium fly ash geopolymer concrete suitable for ambient curing, Procedia Eng. 125 (2015) 601–607.
[25] P.S. Deb, P. Nath, P.K. Sarker, Drying shrinkage of slag blended fly ash geopolymer concrete cured at room temperature, Procedia Eng. 125 (2015) 594–600.
[26] K. Somna, W. Bumrongjaroen, Effect of external and internal calcium in fly ash on geopolymer formation, in: Developments in Strategic Materials and Computational Design II: Ceramic Engineering and Science Proceedings, vol. 32, 2011, pp. 1–6.
[27] K. Somna, C. Jaturapitakkul, P. Kajitvichyanukul, P. Chindaprasirt, NaOH-activated ground fly ash geopolymer cured at ambient temperature, Fuel 90 (6) (2011) 2118–2124.
[28] S. Thokchom, D. Dutta, S. Ghosh, Effect of incorporating silica fume in fly ash geopolymers, World Acad. Sci., Eng. Technol. 60 (2011) 243–247.
[29] A.M. Rashad, A comprehensive overview about the influence of different admixtures and additives on the properties of alkali-activated fly ash, Mater. Des. 53 (2014) 1005–1025.
[30] ASTM C618, Standard Specification for Coal Fly Ash and Raw or Calcined Natural Pozzolan for Use in Concrete, ASTM International, West Conshohocken, PA, USA, 2003.
[31] ASTM C989, Standard Specification for Slag Cement for Use in Concrete and Mortars, ASTM International, West Conshohocken, PA, USA, 2014.
[32] ASTM C1240, Standard Specification for Silica Fume Used in Cementitious Mixtures, ASTM International, West Conshohocken, PA, USA, 2003.
[33] ASTM C150, Standard Specification for Portland Cements, ASTM International, West Conshohocken, PA, 2003.
[34] ASTM C33. Standard Specification for Concrete Aggregates. West Conshohocken, USA, 2005.
[35] ASTM C305, Standard Practice for Mechanical Mixing of Hydraulic Cement Pastes and Mortars of Plastic Consistency, ASTM International, West Conshohocken, PA, 2012.
[36] ASTM C1437. Standard Test Method for Flow of Hydraulic Cement Mortar. 2001.
[37] ASTM C109. Standard Test Method for Compressive Strength of Hydraulic Cement Mortars (Using 2-in. or [50-mm] Cube Specimens), 2001.
[38] ASTM C215. Standard test method for fundamental transverse, longitudinal, and torsional resonant frequencies of concrete specimens. Dynamic Young's Modulus, 2008, pp. 5–6.
[39] AASHTO TP95-11. Standard Method of Test for Surface Resistivity Indication of Concrete's Ability to Resist Chloride Ion Penetration." AASHTO Provisional Standards, 2011 Edition. 2011.
[40] ASTM C1202, Standard Test Method for Electrical Indication of Concrete's Ability to Resist Chloride Ion Penetration, ASTM International, West Conshohocken, PA, 2012.
[41] A. Noushini, A. Castel, The effect of heat-curing on transport properties of low-calcium fly ash-based geopolymer concrete, Constr. Build. Mater. 112 (2016) 464–477.
[42] M.L. Wilson, S.H. Kosmatka, Design and control of concrete mixtures, High-Perform. Concr. 15 (2011) 299.
[43] M.Z. Khan, Y. Hao, H. Hao, Synthesis of high strength ambient cured geopolymer composite by using low calcium fly ash, Constr. Build. Mater. 125 (2016) 809–820.
[44] A. Buchwald, H. Hilbig, C. Kaps, Alkali-activated metakaolin-slag blends—performance and structure in dependence of their composition, J. Mater. Sci. 42 (9) (2007) 3024–3032.
[45] S. Kumar, R. Kumar, S.P. Mehrotra, Influence of granulated blast furnace slag on the reaction, structure and properties of fly ash based geopolymer, J. Mater. Sci. 45 (3) (2010) 607–615.
[46] G. Görhan, R. Aslaner, O. Şinik, The effect of curing on the properties of metakaolin and fly ash-based geopolymer paste, Compos. B Eng. 97 (2016) 329–335.
[47] T. Yang, H. Zhu, Z. Zhang, Influence of fly ash on the pore structure and shrinkage characteristics of metakaolin-based geopolymer pastes and mortars, Constr. Build. Mater. 153 (2017) 284–293.
[48] R.R. Lloyd, J.L. Provis, J.S. van Deventer, Microscopy and microanalysis of inorganic polymer cements. 1: remnant fly ash particles, J. Mater. Sci. 44 (2) (2009) 608–619.
[49] F.N. Okoye, S. Prakash, N.B. Singh, Durability of fly ash based geopolymer concrete in the presence of silica fume, J. Cleaner Prod. 149 (2017) 1062–1067.
[50] P. Duan, C. Yan, W. Zhou, Compressive strength and microstructure of fly ash based geopolymer blended with silica fume under thermal cycle, Cem. Concr. Compos. 78 (2017) 108–119.
[51] Y. Ma, Microstructure and Engineering Properties of Alkali Activated Fly Ash-as an Environment Friendly Alternative to Portland Cement, 2013.
[52] Z. Pan, J.G. Sanjayan, B.V. Rangan, Fracture properties of geopolymer paste and concrete, Mag. Concr. Res. 63 (10) (2011) 763–771.
[53] J.K. Su, C.C. Yang, W.B. Wu, R. Huang, Effect of moisture content on concrete resistivity measurement, J. Chin. Inst. Eng. 25 (1) (2002) 117–122.
[54] Q.F. Liu, J. Yang, J. Xia, D. Easterbrook, L.Y. Li, X.Y. Lu, A numerical study on chloride migration in cracked concrete using multi-component ionic transport models, Comput. Mater. Sci. 99 (2015) 396–416.
[55] Q. Zeng, K. Li, T. Fen-Chong, P. Dangla, Pore structure characterization of cement pastes blended with high-volume fly-ash, Cem. Concr. Res. 42 (1) (2012) 194–204.
[56] N.K. Lee, G.H. An, K.T. Koh, G.S. Ryu, Improved reactivity of fly ash-slag geopolymer by the addition of silica fume, Adv. Mater. Sci. Eng. 2016 (2016).
[57] P. Halamickova, R.J. Detwiler, D.P. Bentz, E.J. Garboczi, Water permeability and chloride ion diffusion in Portland cement mortars: relationship to sand content and critical pore diameter, Cem. Concr. Res. 25 (4) (1995) 790–802.
[58] L.O. Nilsson, Durability concept; pore structure and transport processes, in: Advanced Concrete Technology, 2003, pp. 2.